Journal of Sound and Vibration (2002) **254**(5), 927–938
doi:10.1006/jsvi.2001.4137, available online at http://www.idealibrary.com on IDEAL®

INTERACTION BETWEEN A LIQUID LAYER AND VIBRATING PLATES: APPLICATION TO THE DISPLACEMENT OF LIQUID DROPLETS

J. Scortesse, J. F. Manceau and F. Bastien

Laboratoire de Physique et Métrologie des Oscillateurs du CNRS associé à l'Université de Franche-Comté, 32 Avenue de l'Observatoire, 25044 Besançon, France.
E-mail: fbastien@lpmo.edu

(*Received* 19 *March* 2001, *and in final form* 8 *October* 2001)

Various experiments have been performed to study the interaction of a liquid layer and vibrating plates. A liquid layer deposited on a vibrating plate exhibits a deformation of the surface with a high amplitude of vibration (larger than 1 μm at 30 kHz). Furthermore, a water droplet placed on the vibrating plate moves towards an antinode of vibration. These non-linear phenomena are explained by the action of acoustic radiation pressure. An application to the displacement of droplets is presented.

1. INTRODUCTION

Various works describe the interaction of an ultrasonic beam with bubbles, with suspended droplets (see, e.g., those of Cinbis *et al.* [1], Watanabe *et al.* [2]). There are also studies on the interaction of vibration with powder [3]. Recently, Hashimoto *et al.* in 1996 [4] and in 1997 [5] have presented work on the acoustic levitation of planar specimen using lexural vibrations.

We investigate the interaction of the acoustic field produced by a flexural vibration and liquids. The interaction of solids and flexural waves is well known, and has been mainly studied for application to piezoelectric motors since 1982. However, the principles used for the analysis of this kind of interaction cannot be extended to the solid–liquid interaction. In this work, it is shown experimentally that a displacement of a water drop on the vibrating surface of a horizontal stator can be achieved. This experiment requires a high amplitude of vibration and a control of the wetting of the drop. In order to understand better the interaction of a fluid and a vibrating plate, experiments have also been performed with a thin layer of fluid on the vibrating structure. An interpretation of these observations based on an acoustic radiation pressure concept will be presented.

2. INTERACTION BETWEEN A WATER LAYER AND A VIBRATING PLATE

A vibrating rectangular plate is assumed to be excited at a resonant frequency, with a thin layer of water deposited on the plate. As can be seen from Figure 1, the surface of the water layer is modified, with bumps appearing at the position of antinodes and with valleys

0022-460X/02/$35.00

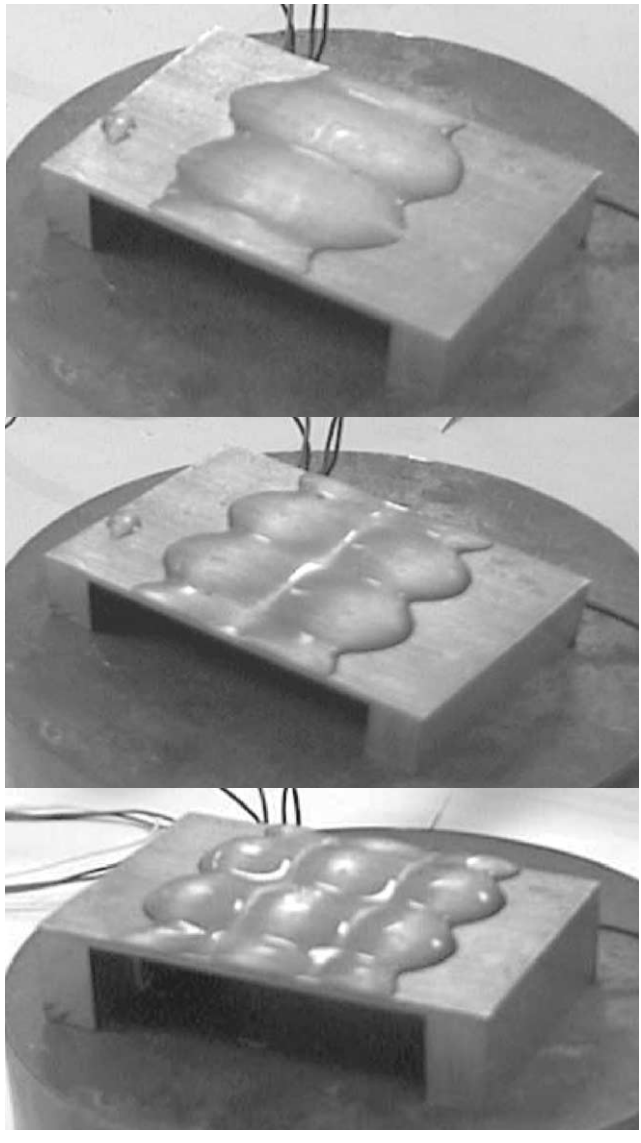

Figure 1. Images of modes with water on a vibrating rectangular membrane. Top: mode (2,3); middle: mode (3,3), bottom: mode (4,3).

forming along nodal lines. Obviously, the surface evolves as the vibrating modes are modified when the frequency is varied. Figure 1 shows three cases corresponding to modes (2,3), (3,3) and (4,3). In this modal classification, the first and second digits are, respectively, the number of nodes along the Ox-axis and along the Oy-axis.

In order to obtain easily the profile of the surface, the experiment is achieved using a "caterpillar" like structure. This structure is made up of a beam closed on itself, in order to produce a continued structure (component). This type of component allows the production of a standing wave at any position, since the structure has no ends. The vibration is excited with four piezoelectric ceramics (see Figure 2). Two ceramics on the left side are used to excite a given standing wave. The other ceramics pair can be used to excite another standing

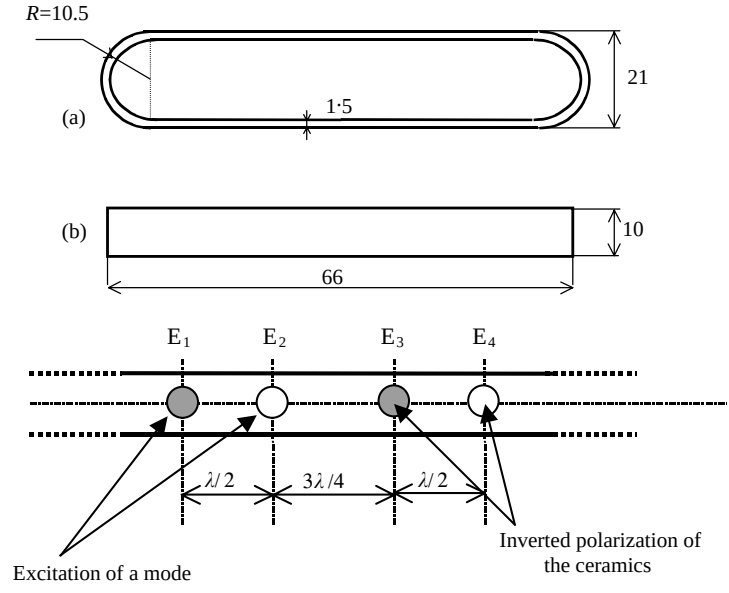

Figure 2. Sketch of the "carterpillar" actuator and position of ceramics. (a) Side view; (b) top view.

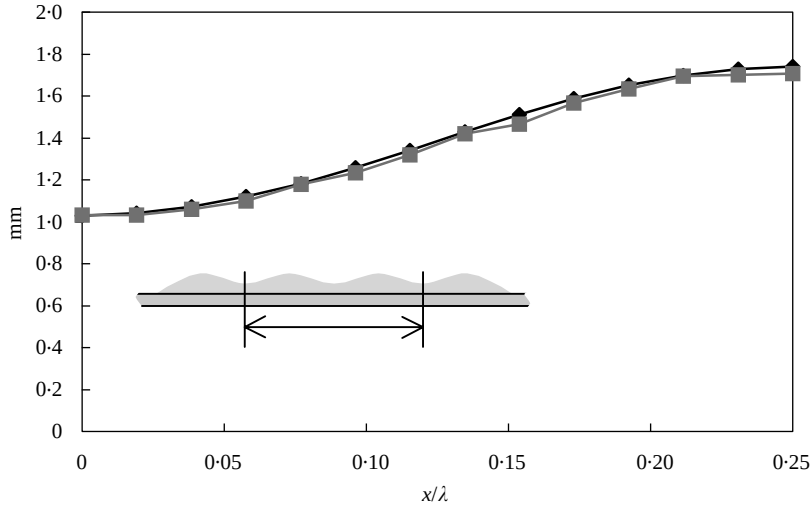

Figure 3. From experiment and fit profile of the water surface (for a quarter of wavelength) as a function of x/λ.

wave, shifted by a quarter of a wavelength. This shift is also the maximum drop displacement step that can be achieved. This is because the drop can move towards the antinode of the beam vibration, as will be described later.

The structure can also be used with a liquid layer. In this case, when the surface is vibrating, the liquid surface is modified. A typical experimental profile as a function of x/λ along the Ox-axis is shown in Figure 3. A good fit to this profile is obtained with the function

$$z(x) = a_0 + a_1 \sin^2(kx). \tag{1}$$

For the device shown in Figure 2, fitted, the coefficients are $a_0 = 1{\cdot}03 \times 10^{-3}$ m, $a_1 = 0{\cdot}71 \times 10^{-3}$ m, $k = 0{\cdot}345 \times 10^3\,\mathrm{m}^{-1}$. The initial depth of the liquid layer is $1{\cdot}4 \times 10^{-3}$ m and the vibration frequency of the beam is 28·7 kHz.

3. EFFECT OF THE ACOUSTIC RADIATION PRESSURE.

In order to understand the observations reported in the previous section, a physical argument is introduced to explain the permanent deformation of the water surface. The most favourable theory to explain the experimental results seems to be the acoustic radiation pressure. It is shown here that this theory can explain both the deformation of a free liquid layer and the displacement of a water droplet.

3.1. MODIFICATION OF THE SURFACE WATER LAYER

A model has been developed (see reference [6]) taking into account the hydrostatic pressure, the capillary pressure induced by the surface tension σ and the radiation pressure. Fundamentals on radiation pressure and acoustic streaming can be found in references [7–9]. A water layer on the "caterpillar" structure is considered. The profile of water surface is given by the function $z(x)$ in equation (1).

The capillary pressure P_c (see reference [10]) is according to the Laplace law

$$P_c = P_{in} - P_{out} = \sigma\left(\frac{1}{R_x} + \frac{1}{R_y}\right), \tag{2}$$

where P_{in} and P_{out} are the pressures inside and outside the layer, σ is the surface tension, and R_x and R_y are the curvature radii. For the evaluation of $1/R_x$, it is considered that $ka_1 \ll 1$ (see equation (1)) leading to $z'(x) \ll 1$. R_x can then be expressed as

$$R_x \approx -1/z''(x). \tag{3}$$

Moreover, as a first approximation, the curvature radius in a plane perpendicular to Oy is supposed to be constant. If the section is supposed to be elliptical then

$$R_y = w^2/4z(x), \tag{4}$$

where w is the width of the structure. This approximation is sufficient for a width of 1 cm. The hydrostatic pressure has also to be taken into account. The acoustic radiation pressure as a function of x is denoted $P_r(x)$, which is given by

$$P_{in} = P_{ref} - \rho g z(x) + P_r(x), \tag{5}$$

where P_{ref} is the reference pressure in the liquid layer: that is to say the pressure at the interface between the water and the vibrating structure. It is assumed that near the surface, P_{out} is equal to the ambient pressure P_0. Then equation becomes, with g the gravity acceleration,

$$\rho g z(x) + \sigma\left(\frac{4z(x)}{w^2} - z(x)\right) = P_r(x) + P_{ref} - P_0. \tag{6}$$

with $z(x)$ expressed as found in the "caterpillar" experiment function. An identification of terms including $\sin^2 kx$ yields the relation

$$\left[\rho g + 4k^2\sigma + \frac{4\sigma}{w^2}\right] a_1 \sin^2(kx) = P_r(x). \tag{7}$$

Therefore, the experimental determination of a_1 gives $P_r(x)$. In order to verify the accuracy of this approach, P_r is evaluated as a function of the excitation level. The pressure of vibration is given by [6]

$$P_r(x) = \rho c^2 \frac{(2 + B/A)}{2} \left\langle \left(\frac{\partial u}{\partial z} \right)^2 \right\rangle, \tag{8}$$

where A and B are non-linear parameters of water [11], $\langle . \rangle$ denotes temporal averaging, and z is the direction of propagation in water. With propagation in the z direction

$$u(x, z, t) = u_0 \sin(kx) \cos(kz - \omega t).$$

Then

$$P_r(x) = \tfrac{1}{4} \rho \omega^2 u_0^2 (2 + B/A) \sin^2(kx). \tag{9}$$

If the non-linear parameters are not taken into account, the last equation can be reduced to

$$P_r(x) = (v/c) P, \tag{10}$$

where v is the particle velocity, c is the sound speed, and P is the acoustic pressure.

With $\sigma = 72 \times 10^{-3}\,\mathrm{J/m^2}$, $B/A = 5{\cdot}2$, $w = 1\,\mathrm{cm}$, $\omega = 1{\cdot}79 \times 10^5\,\mathrm{rad/s^1}$, $\rho = 10^3\,\mathrm{kg/m^3}$, $a_1 = 0{\cdot}71 \times 10^{-3}\,\mathrm{m}$, $k = 0{\cdot}345 \times 10^3\,\mathrm{m^{-1}}$, the amplitude of vibration is calculated from equations (7) and (9) to be $u_0 = 0{\cdot}76 \times 10^{-6}\,\mathrm{m}$. This amplitude of vibration is close to the amplitude measured with an optical interferometer on the vibrating structure without the liquid (about 10^{-6} m). This is a verification of the role of the acoustic radiation pressure.

3.2. WATER DROPLET DISPLACEMENT

A drop of liquid on a plane is now considered. Upon assuming that the acoustic radiation pressure as a function of the abscissa x is known (with the position of the antinode settled at $x = 0$),

$$P_r(x) = P_{0r} \sin^2 kx, \tag{11}$$

where $k = 2\pi/\lambda$ is the wavelength number.

This approximation is useful to appreciate the required vibration level, and to find the best conditions for the displacement of a droplet. In a first approximation, the droplet is assumed to be a segment of a sphere. The radius of the sphere is R, the radius of the water contact area is r and φ_0 is the contact angle. Then

$$r = R \sin \varphi_0.$$

It is simple to compute P_r as a function of R, θ, φ and x_0, x_0 being the position of the top of the droplet and θ and φ_0 being the angles shown in Figure 4.

Then the resulting force produced by the acoustic radiation pressure on this liquid drop can be evaluated. The force F_X along Ox-axis is obtained by integration

$$F_X = \int_0^{\varphi_0} \int_0^{2\pi} P_r(R, \theta, \varphi, x_0)\, R^2 \sin^2\varphi \cos\theta \, \mathrm{d}\theta \, \mathrm{d}\varphi. \tag{12}$$

The normalized variables $K_r = r/\lambda$ and $K_p = x_0/\lambda$ are then introduced, so that $P_r(R, \theta, \varphi, x_0)$ can be rewritten as

$$P_r(R, \theta, \varphi, x_0) = P_{0r} \sin^2 k(R \cos\theta \sin\varphi + x_0) = P_{0r} \sin^2 2\pi \left[K_r \frac{\cos\theta \sin\varphi}{\sin\varphi_0} + K_P \right]. \tag{13}$$

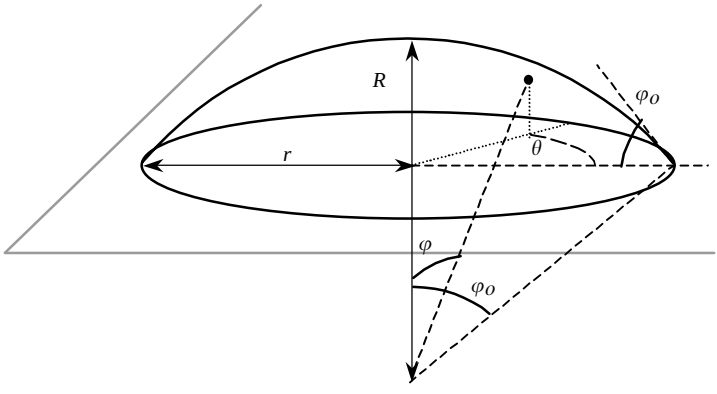

Figure 4. Sketch of the drop on a horizontal surface.

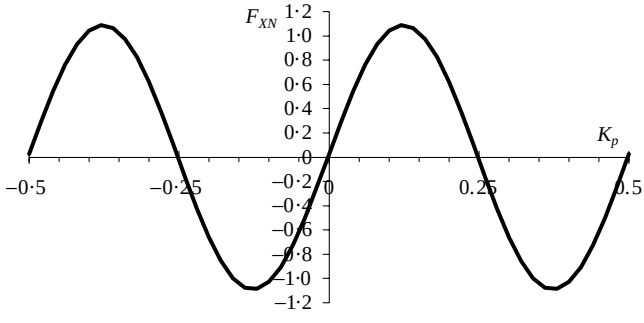

Figure 5. Normalized force F_{XN} as a function of the normalized droplet position.

Then equation (12) becomes

$$F_X(K_r, K_P, \varphi_0) = \frac{P_{0r}}{k^2} \int_0^{\varphi_0} \int_0^{2\pi} \sin^2\left(2\pi\left[K_r \frac{\cos\theta \sin\varphi}{\sin\varphi_0} + K_P\right]\right) \frac{4\pi^2 K_r^2}{\sin^2\varphi_0} \sin^2\varphi \cos\theta \, \mathrm{d}\theta \, \mathrm{d}\varphi. \tag{14}$$

F_{XN} can be introduced as

$$F_X(K_r, K_P, \varphi_0) = \frac{P_{0r}}{k^2} F_{XN}(K_r, K_P, \varphi_0). \tag{15}$$

As an example F_{XN} is computed for $\varphi_0 = \pi/3$ and $K_r = 0{\cdot}2$ as a function of K_P in the range $-0{\cdot}5$ to $0{\cdot}5$. The curve in Figure 5 shows that the drop is in an unstable equilibrium at the node position ($K_P = 0$) and in a stable equilibrium at the antinode position ($K_P = 0{\cdot}25$). A maximum for the force is found at $K_P = 0{\cdot}125$.

In Figure 6, F_{XN} is plotted as a function of K_r for $K_p = 0{\cdot}125$ and for several values of the contact angle φ_0. It can be observed that the force increases as φ_0 and that the optimum value of K_r is close to $0{\cdot}25$.

It is possible to compute the volume of the drop as a function of r and φ_0. Then F_X can be calculated as a function of P_{0r}, K_P, k, φ_0 and of the volume of the drop (vol). For $K_P = 0{\cdot}125$, $vol = 0{\cdot}4 \times 10^{-8}$ m^3, $k = 314$ m^{-1} ($\lambda = 0{\cdot}02$ m) and $P_{0r} = 1$ Pa, F_X is plotted as a function of φ_0. It can be seen that the force increases with φ_0 (Figure 7).

F_X is plotted as a function of the droplet volume in Figure 8 for $K_P = 0{\cdot}125$, $\lambda = 0{\cdot}02$ m, $\varphi_0 = \pi/2$ and $P_{0r} = 1$ Pa. An optimum volume maximizing the force is seen to exist.

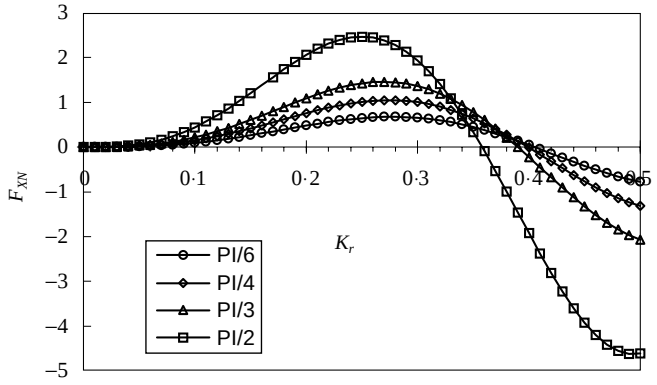

Figure 6. Normalized force F_{XN} as a function of K_r for several values of φ_0.

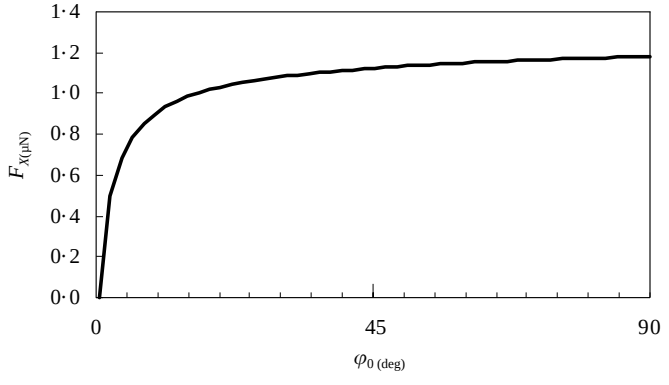

Figure 7. Force F_X as a function of φ_0.

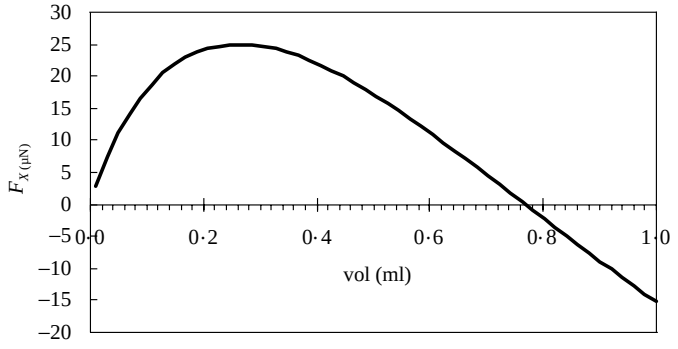

Figure 8. Force F_X as a function of the droplet volume.

One can now evaluate the minimum value P_{0r}^m of P_{0r} required to move the droplet. The condition is that the work of the force along a displacement Δx must be at least equal to the work required to remove the liquid from the part of the wet surface that becomes dry. Therefore, if the work of adhesion for a unit of surface W_{12} is given by [12]

$$W_{12} = \sigma(1 + \cos\varphi_0), \tag{16}$$

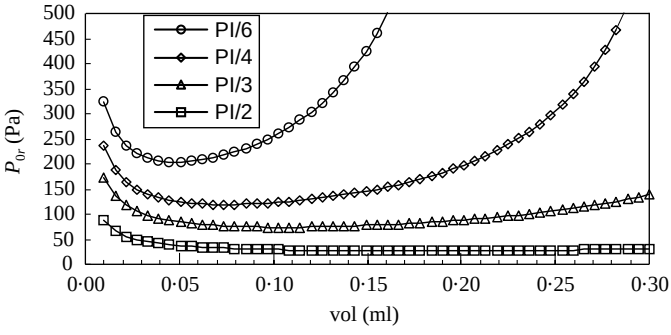

Figure 9. Pressure P_{0r}^{m} as a function of the volume for several values of contact angle φ_0.

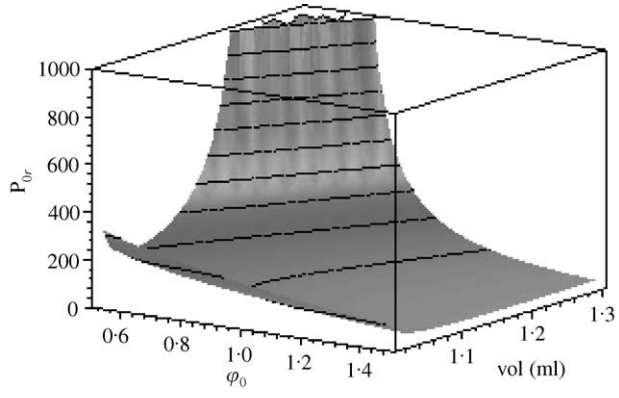

Figure 10. Pressure P_{0r}^{m} as a function of the volume and φ_0.

where σ is the surface energy of the liquid, then equating of the work leads to

$$\sigma(1 + \cos\varphi_0)2rx\Delta x = F_X\,\Delta x = \frac{P_{0r}^{m}}{k^2}F_{XN}\,\Delta x. \tag{17}$$

Then

$$P_{0r}^{m} = \frac{\sigma(1 + \cos\varphi_0)}{F_{XN}}k^2. \tag{18}$$

With $K_P = 0{\cdot}125$, $\lambda = 0{\cdot}02$ m, the last equation can be rewritten as a function of the volume and of φ_0 (Figures 9 and 10). It can be seen that the required displacement is much easier to obtain for large values of φ_0 and that the operating range of the volume is around 0·1 ml for $\lambda = 0{\cdot}02$ m.

Furthermore, $P_{0r}^{m} = C_1\,A^2\,\omega^2$, where A is the amplitude of the vibration used to produce the radiation pressure, C_1 is a constant and $\omega = 2\pi f$ (with f the frequency).

Figure 11 shows the minimum value of the amplitude A that is required to move the droplet as a function of the volume. Figure 12 displays the same as a function of both volume and φ_0.

One can now investigate the influence of the frequency. When K_r, K_P and φ_0 are the given data, then

$$F_X = f(K_P, \varphi_0, K_r)\frac{P_{0r}}{k^2} \tag{19}$$

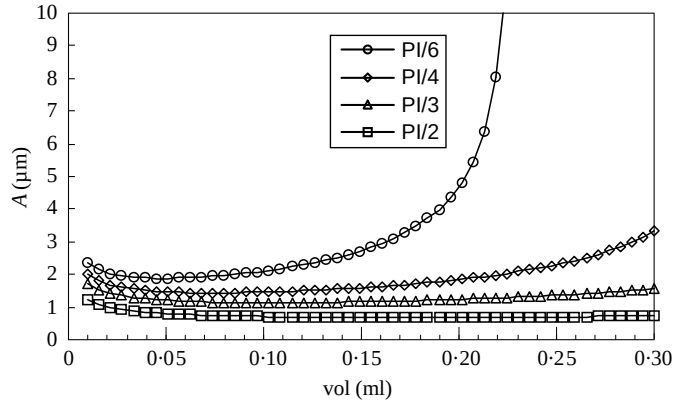

Figure 11. Minimum amplitude of vibration required to move the droplet as a function of the volume for several values of contact angle φ_0.

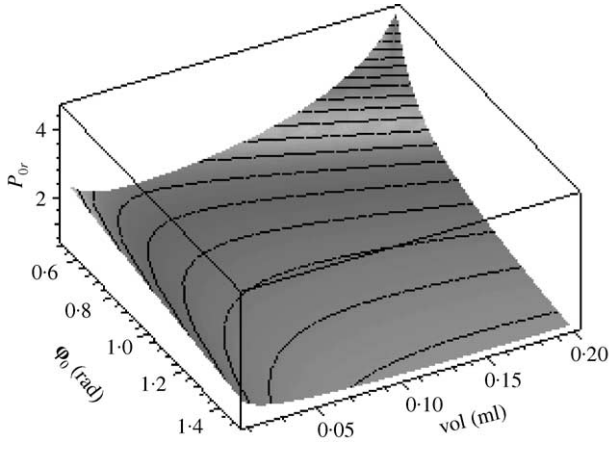

Figure 12. Minimum value of the amplitude A in order to move the droplet as a function of volume and φ_0.

and

$$F_X = \sigma(1 + \cos\varphi_0)\,2r = 2\sigma(1 + \cos\varphi_0)K_r 2\pi/k. \tag{20}$$

Then

$$P_{0r}^m = f_2(K_P, \varphi_0, K_r, \sigma)k. \tag{21}$$

On the other hand,

$$P_r = C_1\omega^2 A^2 \sin^2 kx. \tag{22}$$

Then

$$P_{0r}^m = C_2\omega^2 A^2, \tag{23}$$

where C_1 and C_2 are two constants.

If the radiation pressure is produced by a flexure wave, such as the A_0 Lamb wave mode, then for a thin plate ($e/\lambda \ll 1$, e being the plate thickness) ω is proportional to k^2, and therefore

$$P_{0r}^m = C_3 k^4 A^2 = f_2(K_r, K_P, \varphi_0, \sigma)k. \tag{24}$$

Then $A \propto k^{-3/2}$ or $A \propto \omega^{-3/4}$.

For the efficiency to remain a constant as the frequency increases, the quantity $Q = A\,\omega^{3/4}$ has to be made a constant.

Usually, for a given device, the amplitude A decreases with the frequency, and often $A\omega$ remains a constant. In that case, Q is proportional to $\omega^{-1/4}$. As the quantity Q decreases slowly with frequency, an increase in the frequency is not always favourable. Nevertheless, if the frequency increases, then there is a decrease of the wavelength λ and the optimum of action is obtained for a smaller droplet.

To sum up, due to acoustic pressure the model shows that it is possible to move droplets with dimensions dictated by the wavelength. However, the contact angle has to be not too small to prevent too large an adhesion of the droplet onto the substrate.

4. APPLICATION

Experimentally, it has been observed that a droplet that is not located at an antinode position moves towards an equilibrium position, i.e., the nearest antinode, when a standing wave is generated with sufficiently high vibration amplitude.

A possible application of this phenomenon is the continuous displacement of a water droplet by using a moving standing wave. Let us describe the principle of antinode displacement. On the caterpillar, ceramics E_1 and E_2 depicted in Figure 2 are supplied with an in-phase sinusoidal voltage. At first approximation, these ceramics excite a standing wave in the structure. With the abscissa origin positioned at the centre of E_2, the amplitude of the flexural wave is given by

$$\Psi_1 = A_1 \cos kx \cos \omega t, \tag{25}$$

with $k = 2\pi/\lambda$ and $\omega = 2\pi f$ (f = frequency and λ = wavelength).

The second group of ceramics (E_3 and E_4) excites another standing wave with an amplitude Ψ_2 given by

$$\Psi_2 = A_2 \cos(kx + 3\pi/2) \cos \omega t = -A_2 \sin \mathrm{k}x \cos \omega t. \tag{26}$$

Upon introducing the parameter β defined by $A_1 = A'_1 \cos\beta$ and $A_2 = A'_2 \sin\beta$, the resulting amplitude is

$$\Psi = \Psi_1 + \Psi_2 = [A'_1 \cos\beta \cos kx - A'_2 \sin\beta \sin kx] \cos \omega \mathrm{t}. \tag{27}$$

If $A'_1 = A'_2$, the previous relation can be rewritten as

$$\Psi = [A' \cos\beta - kx)] \cos \omega t. \tag{28}$$

The nodal line position x_0 is obtained by solving

$$\beta - kx_0 = \pi/2 + m\pi \quad (m\text{: integer}), \tag{29}$$

which corresponds to

$$x_0 = \frac{\beta}{k} - \left(\frac{\lambda}{4} + m\frac{\lambda}{2}\right). \tag{30}$$

The position x_0 varies with β linearly. As the force applied to the liquid has a period of $\lambda/2$ (see Figure 5), β/k can be chosen between zero and $\lambda/2$. In fact, it is difficult to get exactly $A'_1 = A'_2$ because the vibration amplitude is not only a function of the level of the applied voltage, but also a function of other parameters such as the coupling between metal and

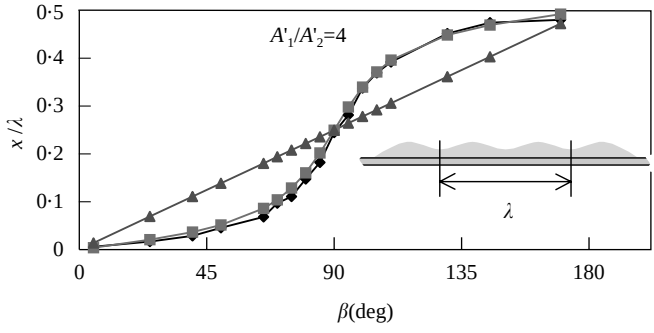

Figure 13. Bubble position as a function of control parameter B from experiment and model.

ceramic. If $A'_1 \neq A'_2$, then the nodal line position x_0 does not vary linearly with β and $x_0 = f(\beta)$ can be easily obtained by solving the equation

$$\frac{A'_1 \cos\beta}{A'_2 \sin\beta} = \tan(kx). \tag{31}$$

The antinode displacement has been experimentally investigated with a water layer on the vibrating actuator. The position is monitored by using an air bubble on the water surface. The bubble displacement is not directly caused by the radiation pressure effect. Indeed, the bubble moves towards a nodal line and not towards an antinodal line, but the movement can be used to show the displacement of the nodal system. Figure 13 gives the antinode position as a function of β. The experimental result is very close to the predicted result with $A'_1/A'_2 = 4$.

This result shows that it is possible to move continuously the nodal line using the caterpillar device. In fact, the practical realization is difficult since in order to move a droplet a high level of vibration is required and the phenomenon is no longer linear. Another difficulty stems from the sensitivity of the droplet displacement method to the variation of the contact angle, which depends on the surface cleanness. With the present device, the movement control is not perfect. Nevertheless, the observed effect is sufficiently important to be considered for an application to the displacement of droplets.

5. CONCLUSION

The possibility to move continuously a drop of water by using a flexural vibration has been observed. The main result is that a drop with a diameter of the order of a quarter of a wavelength (standing wave) can move towards an antinode if the vibration amplitude is sufficiently high (larger than 1 μm at a frequency of about 30 kHz). The displacement of the antinode line produces the drop movement. Nevertheless, several difficulties remain. First, the stability of the required high level of vibrations is disturbed by the temporal evolution of the coupling between metal and ceramics. Second, the wetting of the surface is very sensitive to the surface cleanness.

Furthermore, the level of vibration is close to the level required to spray the drop. This last phenomenon has been observed several times, and is generally explained by the production of a surface wave on the drop. For large amplitudes, this surface wave produces the ejection of very small droplets by a non-linear effect. Despite these difficulties, the method seems promising.

REFERENCES

1. C. Cinbis, N. N. Mansour and B. T. Khuri-Yakub 1993 *Journal of the Acoustical Society of America* **94**, 2365–2372. Effect of tension on the acoustic radiation pressure-induced motion of the water–air interface.
2. T. Watanabe and Y. Kukita 1993 *Physics of Fluids A* **5**, 2682–2688. Translational and radial motions of a bubble in an acoustic standing wave field.
3. K. Yamada, T. Nakagawa and K. nakamura 1993 *Proceedings of the IEEE Ultrasonics Symposium, Baltimore, MD*, 31 *October*–3 *November* 1993, 457–431. Powder transportation by unidirectional ultrasound radiated from a pair of phase-shifted bending vibrators.
4. Y. Hashimoto, Y. Koike and S. Ueha 1998 *Journal of the Acoustical Society of America* **103**, 3230–3233. Transporting objects without contact using flexural traveling waves.
5. Y. Hashimoto, Y. Koike and S. Ueha 1996 *Journal of the Acoustical Society of America* **100**, 2057–2061. Near field acoustic levitation of planar specimens using flexural vibration.
6. S. Biwersi, J. F. Manceau and F. Bastien 2000 *Journal of the Acoustical Society of America* **107**, 661–664. Displacement of droplets and deformation of thin liquid layers using flexural vibrations of structures. Influence of acoustic radiation pressure.
7. R. T. Beyer 1978 *Journal of the Acoustical Society of America* **63**, 1025–1030. Radiation pressure. History of a mislabeled tensor.
8. C. P. Lee and T. G. Wang 1994 *Journal of the Acoustical Society of America* **94**, 1099–1109. Acoustic radiation pressure.
9. J. Lighthill 1978 *Journal of Sound and Vibration* **61**, 391–418. Acoustic streaming.
10. J. Lyklema 1993 *Fundamentals of Interface and Colloid Science—Vol. 1: Fundamentals*, **294**. New York: Academic Press.
11. R. T. Beyer 1960 *Journal of the Acoustical Society of America* **32**, 719–721. Parameter of non-linearity in fluids.
12. J. Isrealachvili 1992 *Intermolecular and Surface Forces*. London: Academic Press, Chapter 15.